Propagation of waves in a cylindrical liquid crystal optical fiber

R.F. Rodríguez* and J.A. Reyes*
Departamento de Física Química, Instituto de Física, Universidad Nacional Auónoma de México
Apartado postal 20-364, 01000 México D.F., Mexico

Recibido el 18 de septiembre de 1998; aceptado el 15 de enero de 1999

We describe analytically the propagation of optical fields in a cylindrical nematic liquid crystal cored waveguide. In the limit of low incident beam energy we calculate the ray trajectories, the cutoff frequency, the maximum number of modes and the propagation constant of the field distributions, for a core with positive dielectric anisotropy (cyanobiphenil). We first compare our calculated values of the propagation constants with recent numerical estimations and show that the agreement is excellent within an error of 0.8%. The field distributions are also compared and we find that the differences between both approaches are larger. We discuss what we belive are the reasons for this discrepancies and comment on the advantanges and limitations of our precedure.

Keywords: Liquid crystals; waveguides; optical fields

Se describe analíticamente la propagación de campos ópticos en una guía de ondas con núcleo líquido cristalino. En el límite de bajas energías incidentes se calculan las trayectorias de rayo, las frecuencias de corte, el máximo número de modos presentes y las constantes de propagación de las distribuciones espaciales de los campos ópticos, cuando el núcleo tiene una anisotropía dieléctrica positiva (cianobifenil). Se comparan los valores calculados de las constantes de propagación con estimaciones numéricas recientes y se muestra que el acuerdo entre ambas es excelente, dentro de un error del 0.8%. También se comparan las distribuciones de los campos y se encuentra que la diferencia entre ambos enfoques son mayores. Se discuten las razones que creemos son las responsables de estas discrepancias y se comentan las ventajas y limitaciones del método propuesto.

Descriptores: Cristales líquidos; guía de ondas; campos ópticos

PACS: 42.65.Jx; 61.30.Gd; 78.20.Jq

1. Introduction

The propagation of a laser beam through a nematic liquid crystal is a phenomenon that exhibits some very unique and highly nonlinear optical properties [1, 2]. It has been experimentally verified that a sufficiently strong linearly polarized laser field induces an orientational transition, the so-called Optical Freedericksz Transition (OFT), in a nematic film [3]. Above the transition threshold, a linearly polarized incident beam distorts the initial alignment by reorienting the molecules against the elastic torques. For a circularly or elliptically polarized beam, also a variety of nonlinear dynamical regimes may arise during the reorientation process [4].

In recent years a great deal of attention has been given to a different aspect of this process, namely, the possibility of producing a wave guiding effect in optical fibers with liquid crystalline cores [5, 6]. The basic idea is to take profit of the nonlinear optical properties of liquid crystals to produce this effect without restoring to the usual mechanism based on total internal reflection.

In a series of papers we have developed an analytical description of the propagation of optical fields in nematic cored plane cells [7–9], nematic droplets [10], and cylindrical waveguides [11, 12]. However, for the cylindrical geometry we, arbitrarily, considered only the case of a core with a negative dielectric anisotropy, $\epsilon_a < 0$, with $\epsilon_a \equiv \epsilon_{\|} - \epsilon_{\perp}$, where $\epsilon_{\|}$, $\epsilon_{\perp}$ denote, respectively, the dielectric constants parallel and perpendicular to the long axis of the molecules. The opposite choice could have been equally plausible, simply we were not aware of any experimental or numerical results, either for positive or negative dielectric anisotropy, to compare with and assess the validity of our approach. Recently we have become aware of interesting numerical work on nematic cylindrical waveguides [5, 6, 13, 14] for the case of a positive birefringence, $\epsilon_a > 0$, a fact that offers the possibility of comparing the results of our analytical approach with the numerical one. Here lies the main motivation of the present work. More specifically, we use the formalism we have developed to compare quantitatively the propagation constants and the field amplitudes calculated analytically but in an approximate way, with the exact but numerical results obtained by Lin *et al.* As will be shown below, our approach offers a better physical insight on the whole propagation process and allows to calculate physical properties of the waveguide, such as dispersion relations, cut-off frequencies or maximum number of guided modes, that are of importance for the design of the guide itself. For this purpose we will quote and use previous results of our own work providing for the specific references where a more detailed derivation of them may be found.

Let us consider a waveguide with a quiescent nematic liquid crystal core confined within a cylindrical region of radius $\mathcal{R}$ and length L, surrounded by an infinite homogeneous isotropic dielectric cladding with dielectric constant ϵ_c, as depicted in Fig. 1. The equilibrium orientational configurations are determined by minimizing the corresponding

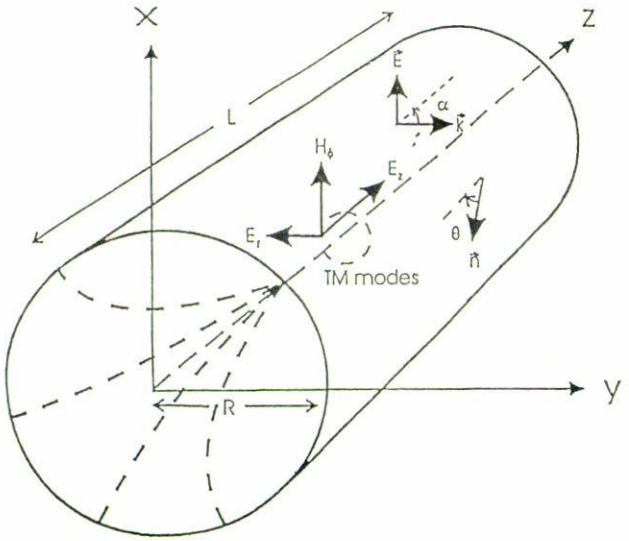

FIGURE 1. Schematic of a linearly polarized laser beam propagating through a nematic liquid crystal cylindrical waveguide.

total Helmholtz free energy functional and we assume that the initial state is given by the so called *scape configuration* [15], $\theta(x) = 2\arctan x$, with $x \equiv r/\mathcal{R}$. Under these conditions a linearly polarized laser beam of amplitude E_0 is incident into the guide with an angle α with respect to the axis of the cylinder. If the optical field is intense enough so that the incident polarization is greater than the orientational transition threshold E_c, the initial state will be distorted by reorienting the director. However, in this work we only consider the case of a low intensity beam where the initial orientation prevails.

The dynamics of the optical field propagating through an anisotropic nematic is described in terms of the corresponding Maxwell's equations without sources. Following the usual procedure [16] it is straightforward to derive the following wave equation for the magnetic field

$$\frac{\epsilon_\perp \epsilon_{\shortparallel}}{c^2}\frac{\partial^2 \vec{H}}{\partial t^2} + \nabla \times \left[\epsilon^{-1} \nabla \times \vec{H}\right] = 0, \tag{1}$$

with a similar equation for $\vec{E}$. The vectors $\vec{D}$ and $\vec{E}$ are related by the following constitutive relation

$$D_i = \epsilon_{ij}[\theta(r)]E_j, \tag{2}$$

where ϵ_{ij} is the spatially varying dielectric permittivity tensor which for an uniaxial nematic is given by

$$\epsilon_{ij} = \epsilon_\perp \delta_{ij} + \epsilon_a n_i n_j$$

where $\vec{n}$ denotes the director field. Furthermore, since for many nematics the magnetic susceptibility is much smaller than the dielectric one, we have assumed a nonmagnetic medium, that is $\vec{B} = \mu_0 \vec{H}$, with $\mu_0 = 1$.

Although the incident beam in general is neither planar or Gaussian, we shall assume that the normal modes within the cavity are cylindrical plane waves propagating along the z axis, namely,

$$E_j(z,r,t) = E_j(r,k_0)\exp\left[i(\beta z - \omega t)\right], \tag{3}$$

$$H_j(z,r,t) = H_j(r,k_0)\exp\left[i(\beta z - \omega t)\right], \tag{4}$$

where the subindex $j = z, r, \phi$ identifies the cylindrical coordinates z, r and ϕ. β is the propagation constant and ω is the angular frequency of the wave. For each value of β there is a specific field distribution described by $E_j(r,k_0)$ and $H_j(r,k_0)$ which remains unchanged with propagation along the guide. These distributions are referred to as the modes of the waveguide.

As will be shown below, for the geometry under consideration it is more convenient to describe the propagation of waves in the fiber in terms of the complete representation provided by the transverse magnetic (TM) and electric (TE) modes [16]. The important issue to emphasize here, is that only the transverse magnetic components E_r, E_z and H_ϕ of the optical field will couple to the reorientation dynamics, while the TE modes do not and may, therefore, be neglected in the description. The TM modes have only one magnetic transverse component and are defined by the conditions $H_z = 0$ everywhere inside the cell and $E_z|_{r=R} = E_z^{\rm cld}|_{r=R}$ on its boundary. Likewise, the corresponding TE modes are E_ϕ, H_r and H_z and satisfy the conditions $E_z = 0$ in every point inside cell and $\partial H_z/\partial z|_{r=R} = \partial H_z^{\rm cld}/\partial z|_{r=R}$ on the fiber boundary; in this case the electric field has only one transverse component.

Substitution of the above expressions for the fields, (3) and (4), into the wave equations for $\vec{E}$ and $\vec{B}$, Eq. (1), leads to the following dimensionless set of equations for the transverse magnetic (TM) modes H_ϕ, E_r and E_z,

$$\epsilon_{rr}\frac{d^2H_\phi}{dx^2} + \left(\frac{\epsilon_{rr}}{x} + \frac{d\epsilon_{rr}}{dx} - 2ipk_0\mathcal{R}\epsilon_{rz}\right)\frac{dH_\phi}{dx} + \left[(k_0\mathcal{R})^2\left(\epsilon_\perp\epsilon_{\shortparallel} - p^2\epsilon_{zz}\right) - \frac{\epsilon_{rr}}{x^2} - ipk_0\mathcal{R}\left(\frac{d\epsilon_{rz}}{dx} + \frac{\epsilon_{rz}}{x}\right)\right]H_\phi = 0, \tag{5}$$

$$E_r = \frac{1}{\epsilon_\perp\epsilon_{\shortparallel}}\left[p\epsilon_{zz}H_\phi + i\frac{\epsilon_{rz}}{k_0\mathcal{R}}\left(\frac{dH_\phi}{dx} + \frac{H_\phi}{x}\right)\right], \tag{6}$$

$$E_z = -\frac{1}{\epsilon_\perp\epsilon_{\shortparallel}}\left[p\epsilon_{rz}H_\phi + i\frac{\epsilon_{rr}}{k_0\mathcal{R}}\left(\frac{dH_\phi}{dx} + \frac{H_\phi}{x}\right)\right], \tag{7}$$

and for the transverse electric (TE) modes

$$\frac{d^2E_\phi}{dx^2} + \frac{1}{x}\frac{dE_\phi}{dx} + \left[(k_0\mathcal{R})^2\left(\epsilon_{\shortparallel} - p^2\right) - \frac{1}{x^2}\right]E_\phi = 0, \tag{8}$$

$$H_r = \frac{pE_\phi}{\epsilon_{\shortparallel}}, \tag{9}$$

$$H_z = -\frac{1}{\epsilon_{\shortparallel}k_0\mathcal{R}}\left(\frac{dE_\phi}{dx} + \frac{E_\phi}{x}\right), \tag{10}$$

where $k_0 = \omega/c$, $p = \beta/k_0$ and $x = r/R$. Note that Eqs. (8), (9) and (10) do not depend on θ and therefore, they are not coupled with the reorientation, as was commented above.

There are two important dimensionless parameters in our description. One of them is $q \equiv E_0^2\mathcal{R}^2/8\pi K$, which is equal to the ratio between the electric, $E_0/8\pi$, and elastic, $KL/\mathcal{R}^2L$, energy densities, where K is the nematic's elastic constant. It measures the strength of the coupling between the director and the optical field. The above mentioned low intensity beam limit is defined by $q \ll 1$. The second relevant dimensionless parameter is $k_0\mathcal{R}$ which allows us to define both, the optical OL and WKB limits. In the former one (OL) all the contributions of order $1/k_0\mathcal{R}$ are neglected so that only a geometrical description of the phase fields is obtained, while in the WKB limit these contributions are taken into account to provide additionally the spatial variations of the field amplitudes.

In Ref. 11 we obtained the eikonal equation and the ray trajectories in the OL [Eq. (23) of Ref. 11], from the equations for the TM mode amplitudes. In that situation where $\epsilon_a < 0$, we showed the existence of a cylindrical caustic at x_c which restricts those regions of the fiber where a trajectory is defined, to the central part of the fiber, that is, $0 < x < x_c$. In contrast, for the case under consideration in this work, $\epsilon_a > 0$, we can show that the position x_c remains the same as in the case for $\epsilon_a < 0$, but the region of the cylinder where the ray trajectory is real is now the outer part of the cylinder, namely, $x_c < x < 1$. The behavior of the trajectories in this case is illustrated in Fig. 2 where we plot two ray trajectories of a beam entering the guide at the interface between a cyanobiphenil core ($\epsilon_a > 0$) and the cladding, with incidence angles $\alpha = 15°$ and $30°$, respectively. It can be seen that in the former case the trajectory does not reach the axis of the cylinder, suggesting a sort of inverse wave guiding effect in which the ray is always confined in the interval $x_c < x < 1$. In contrast, for $\alpha = 30°$ there is no caustic and the ray bends towards the central axis and eventually reaches the other side of the cylinder. In both Figs. 2 we have included as a reference, the trajectory corresponding to the isotropic ($\epsilon_a = 0$) limit represented by the straight lines.

Here, we calculate the amplitudes of the TM modes for the different regions inside the cylinder and in the cladding up to WKB order, since this is the required order to make the comparison with the numerical results later on. It can be shown that for $0 < x < 1/(k_0\mathcal{R})$, that is, in the vicinity of the axis of the cylinder, the amplitude $H_\phi(x, k_0)$ may be well represented by a third order Frobenius expansion [17] in powers of x, that is,

$$H_\phi(x, k_0) = Ae^{if}\left(x + Cx^3 + \dots\right). \tag{11}$$

Therefore, the resulting approximation for $H_\phi(x, k_0)$ is no longer a global one for this geometry and it is not valid in the whole domain. As we shall see below, the main consequence of this fact is to produce a slow converge of the approximation.

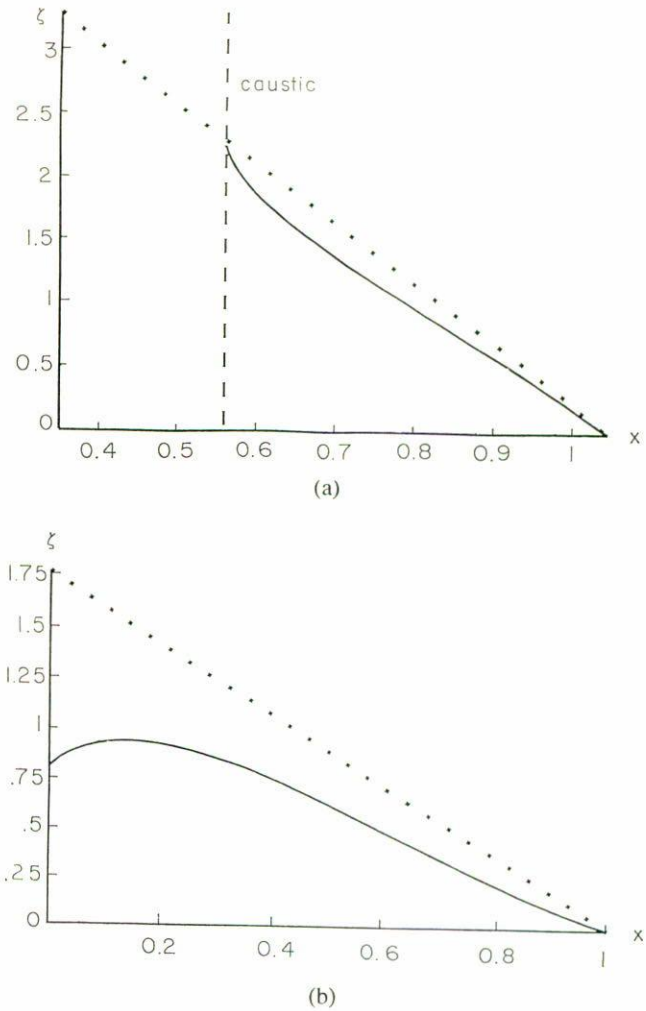

FIGURE 2. a) Ray trajectory for cyanobiphenil for an incidence angle $\alpha = 15°$ (solid line). The broken line corresponds to the isotropic limit with $\epsilon_a = 0$. b) The same as in fig. 2a for $\alpha = 30°$.

Similarly, as the caustic is approached from the central axis, $1/(k_0\mathcal{R}) < x < x_c$, we find that

$$H_\phi(x, k_0) = \frac{A}{\sqrt{x}\,(p_n^2 - \epsilon_{rr})^{\frac{1}{4}}} e^{if} e^{-k_0\mathcal{R}\int_x^{x_c} d\eta\,\Gamma(\zeta, k_0)} \tag{12}$$

and between the caustic and the cladding when $x_c < x < 1$, $H_\phi(x, k_0)$ is given by

$$H_\phi(x, k_0) = \frac{A}{\sqrt{x}\,(\epsilon_{rr} - p_n^2)^{\frac{1}{4}}} e^{if} e^{-k_0\mathcal{R}\int_x^{x_c} d\eta\,\Gamma(\eta, k_0) - \frac{\pi}{2}} \times \cos\left[k_0\mathcal{R}\int_x^{x_c} d\eta\, f(\eta, k_0)\right]. \tag{13}$$

Finally, for the interval $1 < x$ which corresponds to the cladding, we have

$$H_\phi(x, k_0) = \sqrt{\frac{\pi}{2\gamma\mathcal{R}x}} C \exp\left(-\gamma\mathcal{R}x\right). \tag{14}$$

In these equations $\epsilon_{zz} = \epsilon_\perp + \epsilon_a \cos^2\theta$, $\epsilon_{rr} = \epsilon_\perp + \epsilon_a \sin^2\theta$, $\epsilon_{rz} = \epsilon_a \sin\theta\cos\theta$, are the cylindrical components of the dielectric tensor of the nematic, $p_n \equiv \beta/k_0$ and

$f(x,k_0) \equiv i\Gamma(x,k_0)$ is defined by

$$f(x,k_0) = \frac{\sqrt{\epsilon_\perp \epsilon_{\shortparallel}\,(\epsilon_{rr} - p_n^2)}}{\epsilon_{rr}}$$

The constants A, C and γ are to be determined by using the boundary conditions at the nematic cladding interface

$$H_\phi(x=1,k_0) = H'_\phi(x=1,k_0),$$

$$\frac{1}{\epsilon_{\shortparallel} x}\frac{d\left[xH_\phi(x=1,k_0)\right]}{dx} = \frac{1}{\epsilon_c x}\frac{d\left[xH'_\phi(x=1,k_0)\right]}{dx},$$

which requires continuity of the H_ϕ and E_z components. Here the upperscript ($'$) denotes the fields in the cladding.

For the purpose of comparing our analytic but approximate predictions with the exact but numerical results of Ref. 13, we now use the above expressions for $H_\phi(x,k_0)$ to calculate the amplitudes of the first two TM modes $H_{\phi 01}$ and $H_{\phi 02}$ that may exist in the waveguide for the chosen values of the relevant parameters in the numerical approach. For this purpose we use the same value of the parameter $\mathcal{R}/\lambda = 2$ as used in Ref. 13, where λ is the wavelength of the beam in free space. Note that this value amounts to taking $k_0\mathcal{R} = 4\pi \approx 13.6$ in our description. This choice corresponds to the WKB limit, since $k_0\mathcal{R}$ is one order of magnitude larger than 1.

To calculate the modes distributions it is necessary to determine first p_n as a function of the number mode n. This is accomplished by solving the trascendental equation obtained by imposing the boundary conditions at the interface between core and cladding on the above given expressions for $H_\phi(x,k_0)$. This yields

$$\sqrt{\epsilon_{\shortparallel}\epsilon_\perp}\int_{x_c}^{1} d\eta\,\frac{\sqrt{\epsilon_{rr} - p_n^2}}{\epsilon_{rr}} = \frac{n\pi}{k_0\mathcal{R}}, \tag{15}$$

where n is an integer number.

Note that from the definition of ϵ_{rr}, the right hand side of the above equation will be real if $\epsilon_\perp < p^2 < \epsilon_{\shortparallel}$ (strong regime SR); however for $0 < p^2 < \epsilon_\perp$ propagation is still possible (weak regime WR) [7]. From now on we shall restrict ourselves only to the SR case. Then the solution of Eq. (15) is given in Fig. 3 for the same values of the dielectric constants of cyanobiphenil as used in Ref. 6 and for $k_0\mathrm{R} = 4\pi \approx 13.6$. Since $p = \beta/k_0$, from Eqs. (3) and (4) it follows that the condition of propagation of waves along the axis of the cylinder is $p > 0$. In order to obtain the maximum number of propagating modes, recall that when $p_n \equiv \beta/k = 0$ propagation is no longer possible. Therefore, substitution of this condition into Eq. (15) yields the following cutoff frequency ω_{cn}

$$\omega_{cn} = \frac{Qc\pi}{\mathcal{R}}n \tag{16}$$

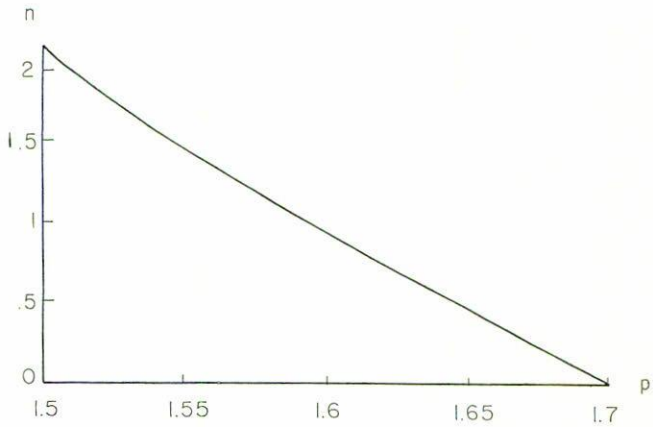

FIGURE 3. Number of modes n as a function of the values of p for which n is an integer.

where we have used the abbreviation

$$Q \equiv \left(\sqrt{\frac{\epsilon_a\epsilon_{\shortparallel}}{\epsilon_\perp}}\ln\sqrt{\frac{\epsilon_{\shortparallel}}{\epsilon_\perp}} - \frac{\epsilon_a}{\sqrt{\epsilon_\perp}}\tanh^{-1}\left(\sqrt{\frac{\epsilon_a}{\epsilon_{\shortparallel}}}\right)\right)^{-1}. \tag{17}$$

From the above expressions it thus follows that the maximum number of propagating modes for a given frequency ω is determined by comparing ω with ω_{cn} . That is, if $\omega_{cm} < \omega < \omega_{c(m+1)}$, the maximum number of modes within the cell is m. Thus, from this inequality and Eqs. (16) and (17) we have

$$m = \frac{Qk_0\mathcal{R}}{\pi}. \tag{18}$$

If we now substitute the numerical values of the material constants of cyanobiphenil on the right hand side of Eq. (17), we find that the maximum number of modes is $m = 2$. Actually, this result is already contained in Fig. 3, which shows that only two modes may propagate simultaneously in the guide. From Fig. 3 it also follows that $p_{n=1} = 1.63$ and since $p_n \equiv \beta c/\omega$, this yields $\beta R = 20.47$. On the other hand, for $P/P_0 = 0$, Fig. 6 in Ref. 6 gives $\beta R = 20.64$; comparing these two values of R yields a difference that amounts to a 0.8% error. We thus conclude that our analytical calculation of the propagation constant is in excellent agreement with the exact numerical result.

Now, the amplitudes of the modes $H_{\phi 01}$ and $H_{\phi 02}$ as functions of x in the WKB limit are obtained from Eqs. (11)–(14) and the values of p_n given in Fig. 3. This yields the curves shown in Fig. 4. Note that the position of the caustic $x_c = 0.56$ is appreciably different from the value given in Ref. 6, which is $x_c = 0.75$. Therefore, in this case the agreement between our results and those in Ref. 6 is not as good as for the propagation constants. We discuss this point below, but before doing this it should be pointed out that in contrast with the numerical method, our formalism allows us to calculate the spatial distribution of the electromagnetic energy density in the WKB limit. This quantity is defined by

$$u_{em}(x,k_0) = \frac{1}{8\pi}\left(\epsilon_{ij}E_iE_j + H_{\phi j}H_{\phi j}\right). \tag{19}$$

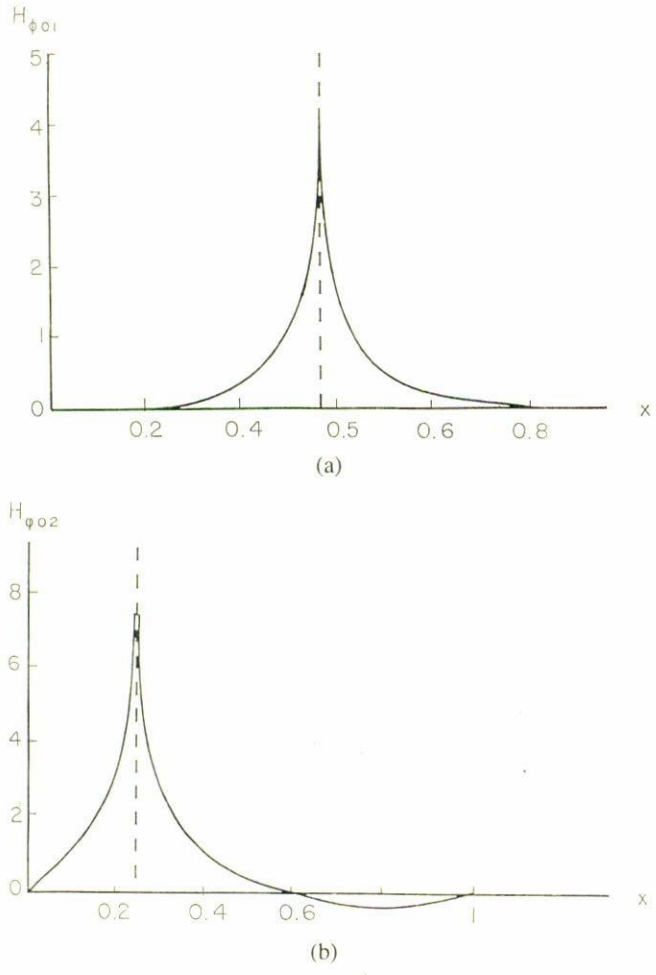

FIGURE 4. a) Amplitude of the TM mode $H_{\phi 01}$ *vs.* the radial coordinate x. b) Same as in Fig. 4a for the mode $H_{\phi 02}$.

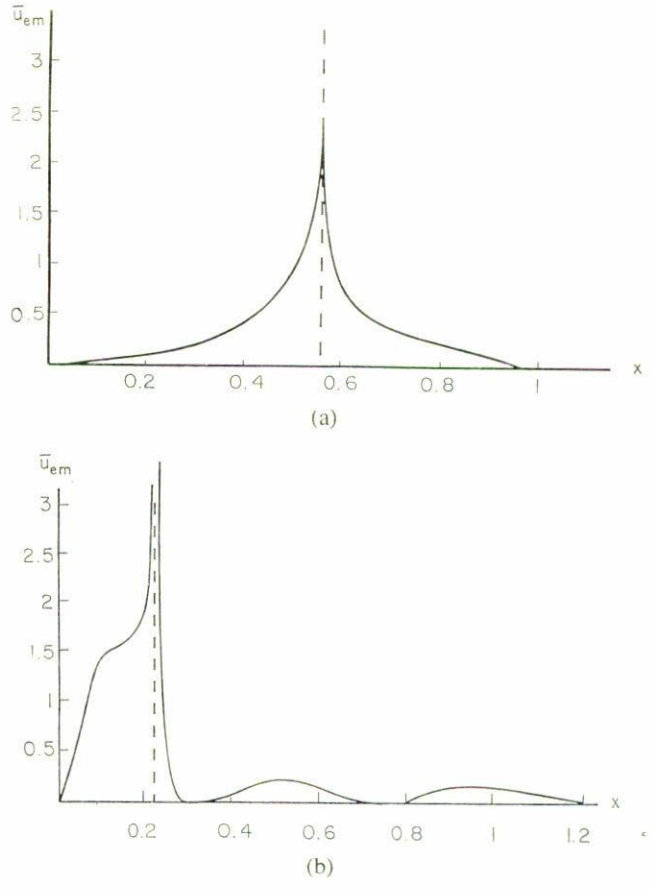

FIGURE 5. a) Normalized electromagnetic energy density $\bar{u} \equiv u/\int_0^\infty 2\pi x u dx$ for the TM mode $H_{\phi 01}$ *vs.* x for cyanobiphenil. It corresponds to an incidence angle $\alpha = 14°$. b) Same as in Fig. 5a for the mode $H_{\phi 02}$. Here the incidence angle is $\alpha = 26°$.

Figures 5 show plots of the normalized energy density $\bar{u} \equiv u/\int_0^\infty 2\pi x u_{em} dx$ as a function of x for both modes $H_{\phi 01}$ and $H_{\phi 02}$. Note that as before, these curves show that the energy is confined within a region around the caustic and not along the central axis of the cylinder, as occurs for the case where $\epsilon_a < 0$ [11].

In summary, in this work we have derived analytical expressions for the ray trajectories in the optical limit and for the amplitudes of the only two allowed modes $H_{\phi 01}$ and $H_{\phi 02}$. We have also obtained explicit expressions for the electromagnetic energy distribution, the cutoff frequency and the maximum number of modes in the cylindrical nematic waveguide. To elaborate on these results and on their comparison with the results of Ref. 6, the following comments may be useful.

First, it should be stressed that our dimensionless and coupled equations for the orientation and field amplitudes contain two parameters with a well defined physical interpretation. The first one, q, measures the strength of the coupling between the nematic and the external field, while the second one, $k_0\mathcal{R}$, defines the optical and WKB limits. Although our calculations were carried out only for the case of a low intensity beam, $q \ll 1$, our approach can be used beyond this limit by carrying out a systematic expansions in powers of $k_0\mathcal{R}$ and q that would allow us to study analytically also the nonlinear case. In this iterative scheme one starts from a director configuration that minimizes the elastic free energy and then use the corresponding dielectric tensor to obtain the distributions of the propagating fields. Then the changes in the dielectric tensor arising from the torques produced by these modes are calculated by solving Eqs. (11)–(14) for the fields again. Actually, this procedure was performed exactly numerically by Lin and Palffy-Muhoray by using an adaptation of the shooting method. However, it should be mentioned that in a previous work we have carried out analytically the first step in this iteration (weakly nonlinear limit) [18, 19] for a planar nematic cell, instead of a cylindrical one. We showed that in that case there may exist propagating optical solitons in the waveguide and it would be of interest to investigate whether the same result holds for the cylindrical geometry considered here. The effects of the hydrodynamic backflows associated with the reorientation have also been considered before [20]

Secondly, we should also point out that in our calculations we used the same value of the expansion parameter

$k_0\mathcal{R} = 13.6$, which was used in the numerical calculations of Lin *et al.* Note that although strictly speaking it is one order of magnitude larger than unity, and that it lies within the interval where the WKB approximation is valid. However, the reason why the calculated amplitudes in the WKB limit behave differently than those in the numerical approach, lies in the fact that these amplitudes are not well defined in the vicinity of the origin. This can be seen by noting that the cylindrical differential equation from which Eqs. (12) and (13) were calculated shows a singularity at the origin. As a result, our approximations (11), (12) and (13) are not well behaved in the neighborhood of the origin. Therefore the approximation (11) looses globality and its convergence decreases. Therefore, since the local behavior of the solution is essential around the origin, the solution of the equation can not be well described by a global approximation. One way of avoiding these difficulties would be to include higher order terms in the development (11), in this case, however, the analytical calculations become more involved. Also, it would be of interest to extend the exact numerical calculations to higher values of $k_0\mathcal{R}$,where the validity of the WKB approximation is better defined and see if the comparison improves.

Thirdly, although our analytical method is an approximate one, it provides for a better physical insight into the mechanisms of propagation along the fiber in terms of more intuitive concepts like optical beam ray trajectories and the analytical expressions for the TM modes. In contrast to the purely numerical method, our approach also allows us to calculate some additional physical properties of the waveguide, such as the waveguide dispersion relation, the cutoff frequency, the maximum number of modes and the spatial distribution of the energy density, which are important in the design of a waveguide.

Acknowledgments

We are indebted with Professor P. Palffy-Muhoray for enlightening discussions on nematic waveguides. We acknowledge partial financial support from Grant DGAPA-UNAM IN105797, México.

---

* Fellow of SNI, México.

1. B.Ya. Zel'dovich, N.F. Pilipotskii, A.V. Sulchov, and N.V. Tabiryan, *JEPT Lett.* **31** (1980) 363.
2. N.Y. Tabiryan, A.V. Sukhov, and B.Ya Zel'dovich, *Mol. Cryst. Liq. Cryst.* **136** (1986) 1.
3. S.D. Durbin, S.M. Arakelian, and Y.R. Shen, *Phys Rev. Lett.* **47** (1981) 1411.
4. E. Santamato, G. Abatte, P. Maddalena, and L. Marrucci, *Phys. Rev. Lett.* **64** (1990) 1377.
5. H. Lin, P. Pallfy-Muhoray, and M.A. Lee, *Mol. Cryst. Liq. Cryst.* **204** (1991) 180.
6. H. Lin and P. Pallfy-Muhoray, *Liq. Cryst.* **14** (1993) 1977.
7. J.A. Reyes and R.F. Rodríguez, *J. Nonlin. Opt. Phys. Mat.* **4** (1995) 943.
8. J.A. Reyes and R.F. Rodríguez, *J. Nonlin. Opt. Phys. Mat.* **6** (1997) 532.
9. R.F. Rodríguez and J.A. Reyes, *Mol. Cryst. Liq. Cryst.* **317** (1998) 135.
10. J.A. Reyes, *Phys. Rev. E* **57** (1998) 6700.
11. J.A. Reyes and R.F. Rodríguez, *Opt. Comm.* **134** (1997) 349.
12. J.A. Reyes, Ph.D. Dissertation, National University of Mexico, 1995 (in Spanish).
13. H. Lin and P.P. Pallfy-Muhoray, *Opt. Lett.* **17** (1992) 722.
14. H. Lin and P. Pallfy-Muhoray, *Opt. Lett.* **19** (1994) 436.
15. P.E. Cladis and M. Kleman, *J. de Physique* **33** (1972) 591.
16. J.D. Jackson, *Classical Electrodynamics*, 2^{nd} Edition, (Wiley, New York, 1986).
17. C.M. Bender and M.C. Arszog, *Advanced Mathematical Methods for Scientists and Engineers*, (Mc Graw Hill, New York, 1978).
18. R.F. Rodríguez and J.A. Reyes, *J. Mol. Liq.* **71** (1997) 115.
19. J.A. Reyes and P. Palffy-Muhoray, *Phys. Rev. E* **58** (1998) 5855.
20. R.F. Rodríguez and J.A. Reyes, *Mol. Cryst. Liq. Cryst.* **282** (1996) 287.